Elsevier Editorial System(tm) for Clinical Neurophysiology
Manuscript Draft

Manuscript Number:

Title: Automated neonatal seizure detection mimicking a human observer reading EEG

Article Type: Full Length Article

Keywords: newborn; seizure detection; electroencephalography (EEG); algorithm

Corresponding Author: Dr. Wouter Deburchgraeve, Ir. Ing.

Corresponding Author's Institution: K.U. Leuven

First Author: Wouter Deburchgraeve, Ir., Ing.

Order of Authors: Wouter Deburchgraeve, Ir., Ing.; Joseph Perumpillichira, MD, DM; Maarten De Vos, Ir.; Renate M Swarte, MD; Joleen H Blok, PhD; Gerard H Visser, MD, PhD; Paul Govaert, MD; Sabine Van Huffel, Prof. Dr. Ir.

Abstract

Objective

The description and evaluation of a novel patient-independent seizure detection for the EEG of the newborn term infant.

Methods

We identified the characteristics of the neonatal seizure by which a human observer is able to detect them. Neonatal seizures were divided into 2 types. For each type, a fully automated detection algorithm was developed based on the identified human observer characteristics. The first algorithm analyzes the correlation between high-energetic segments of the EEG. The second detects increases in low frequency activity with high autocorrelation.

Results

The complete algorithm was tested on multi-channel EEG recordings of 21 patients with and 5 patients without electrographic seizures, totaling 217h of EEG. Sensitivity of the combined algorithms was found to be 88%, Positive Predictive Value (PPV) 75% and the false positive rate 0.66 per hour.

Conclusions

Our approach to separate neonatal seizures into two types yields a high sensitivity combined with a better PPV and much lower false positive rate than previously published algorithms.

Significance

The proposed algorithm significantly improves neonatal seizure detection and monitoring.

* Manuscript

Automated neonatal seizure detection mimicking a human observer reading EEG

W. Deburchgraeve [a], P.J. Cherian [b], M. De Vos [a], R.M. Swarte [c], J.H. Blok [b], G.H. Visser [b], P. Govaert [c] and S. Van Huffel [a]

[a] Department of Electrical Engineering (ESAT), Katholieke Universiteit Leuven, Kasteelpark Arenberg 10 , 3001, Heverlee, Belgium
[b] Department of clinical neurophysiology, Erasmus MC, University Medical Center Rotterdam, 's-Gravendijkwal 230, 3015CE, Rotterdam, the Netherlands
[c] Department of neonatology, Erasmuc MC, University Medical Center Rotterdam, Dr. Molewaterplein 60, 3015 GJ, Rotterdam, the Netherlands

correspondence:
Name: Deburchgraeve Wouter
Telephone number: 0032 498 08 56 76
e-mail: wouter.deburchgraeve@esat.kuleuven.be

keywords: newborn; seizure detection; electroencephalography (EEG); algorithm

Acknowledgements:

- Research Council KUL: GOA-AMBioRICS, CoE EF/05/006 Optimization in Engineering (OPTEC), IDO 05/010 EEG-fMRI, IOF-KP06/11 FunCopt, several PhD/postdoc & fellow grants;
- Flemish Government:
  - FWO: PhD/postdoc grants, projects, G.0407.02 (support vector machines), G.0360.05 (EEG, Epileptic), G.0519.06 (Noninvasive brain oxygenation), FWO-G.0321.06 (Tensors/Spectral Analysis), G.0302.07 (SVM), G.0341.07 (Data fusion), research communities (ICCoS, ANMMM);
  - IWT: PhD Grants;
- Belgian Federal Science Policy Office IUAP P6/04 (DYSCO, `Dynamical systems, control and optimization', 2007-2011);
- EU: BIOPATTERN (FP6-2002-IST 508803), ETUMOUR (FP6-2002-LIFESCIHEALTH 503094), Healthagents (IST–2004–27214), FAST (FP6-MC-RTN-035801), Neuromath (COST-BM0601)
- ESA: Cardiovascular Control (Prodex-8 C90242)

Automated neonatal seizure detection mimicking a human observer reading EEG

Abstract

Objective

The description and evaluation of a novel patient-independent seizure detection for the EEG of the newborn term infant.

Methods

We identified the characteristics of the neonatal seizure by which a human observer is able to detect them. Neonatal seizures were divided into 2 types. For each type, a fully automated detection algorithm was developed based on the identified human observer characteristics. The first algorithm analyzes the correlation between high-energetic segments of the EEG. The second detects increases in low frequency activity with high autocorrelation.

Results

The complete algorithm was tested on multi-channel EEG recordings of 21 patients with and 5 patients without electrographic seizures, totaling 217h of EEG. Sensitivity of the combined algorithms was found to be 88%, Positive Predictive Value (PPV) 75% and the false positive rate 0.66 per hour.

Conclusions

Our approach to separate neonatal seizures into two types yields a high sensitivity combined with a better PPV and much lower false positive rate than previously published algorithms.

Significance

The proposed algorithm significantly improves neonatal seizure detection and monitoring.

1. Introduction

Seizures occur in 1 to 3.5/1000 births and are a common sign of neurological disorder in neonates (Volpe, 2001). The causes of seizures are various, with 90% of all cases being attributed to biochemical imbalances within the CNS, hypoxic ischemic encephalopathy, intracranial hemorrhages and infarcts, intracranial infection, and developmental (structural) anomalies. The newborn brain is very susceptible to seizures as term infants have well-developed excitatory mechanisms and poorly developed inhibitory mechanisms (McBride et al., 2000). This explains that the incidence of seizures is greater in the neonatal period than at any other time in life (Patrizi et al, 2003). There is controversy about whether or not seizures cause brain damage. However, an increasing number of studies have shown that neonatal seizures cause lasting changes in the CNS (Liu et al, 1999; Schmid et al, 1999) and late behavioral effects (Holmes et al, 1998; Koh et al, 1999). In a strategy of neuroprotection of the newborn, effective detection of these seizures is needed in order to assess their potential additional damage and establish timely treatment. The detection of seizures is usually based on clinical signs in conjunction with visual assessment of the EEG. In neonates, the clinical seizures are often subtle and may be missed without constant supervision (Clancy et al, 1988). Furthermore, many seizures tend to be subclinical, implying that they can be detected only by EEG monitoring. Combined with the fact

that EEG analysis requires particular skills which are not always present around the clock in the Neonatal Intensive Care Unit (NICU) this means that many seizures are missed (McBride et al, 2000). Therefore, an automated system that reliably detects neonatal seizures would be of significant value in the NICU.

In the literature, many seizure detection algorithms have been described. The best known methods are based on computing a running autocorrelation function (Liu et al, 1992), rhythmic discharges detection (Gotman et al, 1997), modeling and complexity analysis (Celka et al, 2002), and wave-sequence analysis (Navakatikyan et al, 2006). Others are based on the extraction of features using entropy, wavelets, frequency content, etc., and then training a classifier (Greene et al, 2007; Zarjam et al, 2003; Aarabi et al, 2006) on these features to correctly categorize the EEG. We believe that the classifier approach is not suitable for patient-independent seizure detection. Neonatal seizures have an extremely variable morphology, frequency, and topography, even within the same patient (Lombroso et al, 1996; Shewmon, 1990). Due to this large variability, training a classifier with fixed properties on a set of features is a too rigid strategy.

Our approach to the detection of neonatal seizures is to develop an algorithm which mimics a human observer reading EEG, as it is essentially the human observer we are trying to replace. We identified two major characteristics of neonatal seizures which lead to their detection by a human observer. The first characteristic is that all seizures represent a clear change relative to the background EEG. The second and most important characteristic is the repetitiveness of the signal, because nearly all seizures display some kind of recurrent pattern. We aimed to develop an algorithm based on these two characteristics using time domain signal processing, as this is the most straightforward way to mimic the human observer. The implementation is based on several concepts already introduced in the literature, but we combined and improved these and added some of our own concepts.

2. Methods

2.1 EEG dataset

All data were recorded at the Sophia Children's Hospital (part of the University Medical Center Rotterdam, the Netherlands). The dataset consisted of long-term video-EEG recordings of 26 full-term neonates with perinatal asphyxia of which 21 contained electrographic seizures and 5 were seizure-free. Fourteen had the full 10-20 set of electrodes, while 12 had the restricted 10-20 set of electrodes. Each measurement started within 6 hours from birth. Monitoring was done for 24 to 48 hours. Segments of EEG containing seizures and at least eight hours long were selected for each patient. Sampling frequency was 256 Hz. Inter-rater agreement between two experienced clinical neurophysiologists in scoring seizures in one-hour segments of EEGs from 10 patients was 73%. Subsequently, the data was reviewed jointly by both and the scored seizures were agreed upon by consensus. The 8-hour segments of EEGs were then scored for seizure activity by one of the raters. Seizures were scored when they showed clear variation from the background EEG activity lasting for at least 10 s and showed evolution in time and or change in amplitude and frequency. The dataset consisted of EEGs with a wide variety of background activity, ranging from low voltage, to burst suppression and normal background activity. No selection has been made regarding artefacts present in the EEG. Before analysis the data was filtered between 0.3 and 30Hz and a notch filter at 50 Hz was applied.

2.2 Detection Method

When analyzing the neonatal seizures, we identified two major seizure types. The first type is what we call the spike train seizure type (Fig. 1A); the second is what we call the oscillatory seizure type (Fig. 1B). Nearly all neonatal seizures can be classified uniquely into one of these types or as a combination of the two types (Fig. 1C). In our dataset, roughly 50% of all seizures consisted of a combination of the two types, 35% were purely consisting of spikes and the remaining 15% were pure oscillatory seizures.

(Fig. 1 here)

The major difference between the two types is that the oscillatory type is a fluent, continuous seizure, whereas the spike train type consists of isolated spikes appearing on a background of lower voltage EEG. This means that the oscillatory type has a continuous kind of repetitiveness while the spike train type has a discontinuous kind. Another difference is that the oscillatory activity generally has lower frequency content than the high-frequency spikes.
We need to stress that this categorization into two seizure types is not based on any physiological interpretation, but was adopted purely from a signal processing point of view. A detection algorithm was developed for each seizure type separately. During analysis, both algorithms run in parallel and detection occurs if one or both of the algorithms detects a seizure. The two algorithms are calculated on each EEG-channel separately. When detection occurs in one channel, the complete EEG at that time instance is regarded as seizure activity, independent of the detection result on the other channels. Although the two algorithms differ completely in their implementation, they are closely related and matched to each other.

2.2.1 Detection algorithm for the spike train type

Our human observer approach indicated that the spike train algorithm must detect a *repetitive train* of *isolated spike like segments* of EEG. Accordingly, the algorithm consists of two steps. The first step will isolate the spike like segments and the second will analyze the similarity between these isolated segments.

a. Isolation of the spike like segments.

To detect the local presence of high frequency activity, we use a non-linear energy operator (NLEO) as proposed by Kaiser (1990). The NLEO represents the energy of a discrete time signal, based on the physical energy of the signal producing system. In its discrete form, it is given by:

$$\psi_{kaiser}[x_{(n)}] = x_{(n)}^2 - x_{(n-1)}.x_{(n-2)}$$

With $x_{(n)}$ denoting the current sample of signal x, $x_{(n-l)}$ the first sample before sample n, etc. The key property of this operator is:

$$\psi[A.\cos(\omega_0 n + \vartheta)] = \frac{1}{2}.A^2.\omega_0^2$$

This formula indicates that the output is proportional to the square of both the amplitude and the frequency. In this regard, the NLEO may be considered superior to other energy estimators that simply average the square of the signal and are independent of frequency. Because of these properties, the NLEO amplifies the high-frequency spikes of the spike train relative to the background EEG. A generalized version, which is more robust to noise, is given by Plotkin et al. (1992):

$$\psi[x_{(n)}] = x_{(n-l)}.x_{(n-p)} - x_{(n-q)}.x_{(n-s)},$$

$$l + p = q + s$$

As parameter settings, we used l=1, p=2, q=0, and s=3 (Agarwal et al, 1998). Subsequently, on the output of the NLEO, the root mean square (RMS) was calculated using a moving window of 120 ms and a shift of 1 sample. This value was chosen as a compromise for sensitivity between short spikes (<120 ms) and long spikes (>120 ms). The resulting signal was the smoothed, frequency-weighted energy of the EEG.
Next, this signal was divided into overlapping epochs of 5 s (overlap of 4 s). To each epoch, an adaptive threshold was applied that was defined as:

$$Threshold = 0,6.std(epoch) + q_3(epoch)$$

with 'std(…)' and 'q_3(…)' the standard deviation and 75th percentile of the epoch, respectively. The 75th percentile guarantees that only the highest energy parts of the signal are selected. The standard deviation adapts the threshold to the variability of the signal. Fig. 2 shows an example of the segmentation into high-energy segments of a spike train.

(Fig. 2 here)

The human observer approach requires the spikes to be 'isolated' from the background activity. We implemented this requirement by calculating the spikiness of each high-energetic segment using:

$$Spikiness = \frac{max(segment)}{mean(background)}$$

The background is defined as the EEG with the length of the considered segment just before and after the spike (Fig. 3). Only segments with a minimum length of 60ms and a spikiness higher than 7 were kept.

(Fig. 3 here)

To summarize the segmentation, first those segments which are high-energetic with respect to the complete epoch are detected and next, the spikiness further reduces the number of segments to those which are high-energetic on a very local scale (isolated by comparatively low-energetic EEG).

b. Analysis of the correlation.

Following our human observer's approach, we now have to deal with the repetitive character of the seizures. In time domain processing, repetitiveness (or in this case: similarity between segments) can be estimated using correlation analysis. To detect the occurrence of a repetitive pattern of segments, we developed a correlation scheme that will grow a set of highly correlated segments (Fig. 4). Such a set starts with just one segment and every detected segment of the segmentation step will be used as a starting point for the correlation scheme. In the first step, the cross-correlation of the first segment with the previous segment is calculated. If the maximum value of that cross-correlation is >0.8, that previous segment is added to the set. Next, the preceding segment is selected and the cross-correlation with the two segments of the set is calculated (step 2). If the mean of those two maximum cross-correlations is >0.8, that new segment is also added to set. In case of a repetitive signal, repetition of this process (step 3 etc.) leads to a set of segments which are highly correlated with each other. A detection of a seizure occurs when the number of correlated segments in the set is higher than 6.

(Fig. 4 here)

An important parameter is when to stop the process as it is not efficient to search back for correlated segments indefinitely. This maximum time lag is dependent on the length of the first segment the process started with. Only segments which occur with a time lag less than 40 times the length of the first segment (Fig. 5) are checked.

(Fig. 5 here)

By restricting the time lag based on the length of the first segment, the search is adapted to the length of the correlated segments the algorithm is searching for and thus adapted to the patients EEG. In case the first segment is longer than 0.5 s, the maximum search back length is limited to 20 s. Due to this flexibility, the sensitivity of finding correlated spikes is the same for short as for longer segments (up to 0.5 s).
As this search for correlated segments is calculated for every segment detected in the segmentation step, several (possibly overlapping) sets of correlated spikes will be found in case of a spike-train type seizure. When the spikes of these sets are less than 20 s apart, they are grouped into a single detection. The above process allows for some variation in the morphology of the spikes. The initial correlation must exceed 0.8, which implies a strong similarity. However, when a set starts growing, the similarity may occasionally become less, as only the mean of the correlation with all segments of the set is used. Fig. 6 shows the results of this algorithm. The marked spikes are those that are detected as being part of a spike train type seizure.

(Fig. 6 here)

2.2.2 Detection algorithm for the oscillatory type

A human observer seems to detect oscillatory type seizures as *continuous repetitive activity* that represents an *increase of low frequency activity* relative to the background. In time domain processing, the autocorrelation function is useful for finding a repeating pattern in a signal and, thus, for handling the repetitiveness of oscillator-type seizures. The autocorrelation is the cross-correlation of a signal with a delayed version of itself. Liu et al. (1992) suggested a method based on the autocorrelation function to detect rhythmic discharges in the neonatal EEG. Navakatikyan et al. (2006) have shown that Liu's method displays a high sensitivity but also a high number of false positives. We therefore aimed to develop an autocorrelation-based analysis with a very low false positive rate. This algorithm consists of 2 steps. The first step detects an increase of low-frequency activity and the second analyzes the autocorrelation function of these increases.

a. Detection of an increase in low frequency content.

Every EEG channel is decomposed using the discrete wavelet transform (DWT). The signal is passed through two complementary filters and emerges as two signals. One is the low-frequency component, which is called the approximation, and the other is the high-frequency component or the detail. This process is repeated several times by successive filtering of the approximation. As a result, at each iteration (also called scale) a lower frequency component is extracted. As mother wavelet, we used a biorthogonal wavelet with decomposition order 3, as this wavelet matches the shape of the oscillatory activity we are looking for. The oscillatory activity is most prominent in the δ (0.5-4 Hz) and θ (4-8 Hz) range of frequencies. Therefore, only those wavelet coefficients which correspond to scales of 8-4 Hz, 4-2 Hz and 2-1 Hz are used for further analysis.
Next, the derivative of each selected scale is calculated, and, the result is squared to make it positive and to enlarge differences. To detect significant changes in the resulting signal, a window with a length of 3 s is moved along the signal. Detection occurs if the third quartile of the signal in the window is higher than 2.5 times the third quartile of the previous 30 s of EEG. If a window is detected for a particular scale, the signal in that window represents a significant increase of activity in that specific wavelet sub-band, compared to the background (Fig. 7). This activity is considered potential oscillatory seizure activity.

(Fig. 7 here)

b. Autocorrelation analysis.

At this point, we have detected significant changes of activity in specific wavelet sub-bands of 1-8 Hz. What remains is the analysis of the repetitive aspect of the signal. As described above, our goal is to detect repetitive signals by means of the autocorrelation function. The detected windows in step 1 are divided into 5 s epochs (4 s overlap between epochs) and the autocorrelation function of the epochs is calculated. Fig. 8 shows two examples of epochs with their autocorrelation functions.

(Fig. 8 here)

For our purpose, two features of the autocorrelation function are particularly useful. First, the autocorrelation of an oscillating signal is very symmetric around zero, whereas that of a random signal is not (Fig. 8). To exploit this difference, we calculate the skewness of the autocorrelation. Because of the symmetry, the skewness of the autocorrelation of an oscillating signal will be lower than that of a random signal. The second discriminatory feature compares the percentage difference of intervals between the zero-crossings of the autocorrelation (Fig 9).

(Fig. 9 here)

For the high-activity, low-frequency windows detected in step 1 to be classified as oscillatory seizure, their skewness must be lower than 0.4, and the mean of the interval differences between the zero crossings must be less than 6%.

2.3 Combination of the two detection algorithms

Roughly 50% of the seizures consist of a combination of spike train activity and oscillatory activity. In these cases, both detection algorithms are needed for a complete detection of the seizure. Fig. 10 shows a seizure that starts with oscillatory activity and ends with spike train activity. The oscillation-detection algorithm detects the beginning of the seizure but not the end (Fig. 10A). Conversely, the spike train detection algorithm detects the spike train at the end of the seizure, but not the beginning (Fig. 10B). There is a certain overlap between what is detected by both algorithms (channel Fp1-F3). When the seizure changes from oscillatory to spike train activity, the oscillation becomes spikier but the seizure is still continuous, resulting in detection by both algorithms.
When the results of both algorithms are combined, nearly the complete seizure is detected.

(Fig. 10 here)

A neurologist reading the EEG usually classifies rhythmic EEG activity as a real seizure if it is present for at least 10 s (Shellhaas and Clancy, 2007). To mimic the human observer and to be able to detect these short seizures, we have set the minimum duration in our algorithm to 8 s.

3. Results

Presenting the performance of a seizure detection algorithm is not straightforward. Different ways to measure the performance of an algorithm have been reported in the literature, leading to varying results, which cannot easily be compared. In addition, all these algorithms were tested on different datasets, which makes a comparison even more difficult.
We defined the sensitivity per patient (*SensPP*) as the percentage of seizures marked by the neurologist that are detected.

$$SensPP = (SZ\,\det PP / SZtotPP).100$$

with *SZtotPP* the number of seizures marked by the neurologist for a patient, and *SZdetPP* the number detected by the algorithm for that patient. A seizure was considered as detected when there was a temporal overlap between the marked seizure and the detection.
The total sensitivity for all patients is calculated using 2 methods. The first method simply averages all sensitivities per patient (*SensT_PP*). The second method (*SensT*) measures the percentage of seizures detected of all seizures present in the complete dataset. So, *SensT_PP* measures the expected sensitivity at the patient level and *SensT* at the seizure level. The importance of the difference is that in *SensT_PP,* a patient with only a few seizures is considered to be equally important as a patient with many seizures. *SensT*, on the other hand, regards all seizures as equally important regardless of the patient they occurred in.
The Positive Predictive Value (PPV) is defined as the percentage of detected events that match seizures.

$$PPV = (EVsz / EVtot).100$$

with *EVtot* the total number of detected events and *EVsz* the total number of detected seizures. Occasionally, a single seizure was detected several times by the algorithm. All such events were combined into a single *EVsz* detection. Another useful measure of performance is the number of false positive detections per hour (fp/h). This measure represents an important indicator of the practical usability of the algorithm, because each FP implies that somebody in the NICU will have to check the patient and the raw EEG recording unnecessarily.
The results are given in Table 1.

(Table 1 here)

The *SensT_PP* was 85%, *SensT* was 88%, as the algorithms detected 482 out of 550 seizures present in the dataset. The mean PPV was 75%. There were 143 false positive detections, or 0.66 fp/h. Of all false positives, 45% occurred in 2 of the 26 patients (patient 7 and 23). Closer analysis of these 2 patients revealed that both had low voltage EEG background activity (<15uV) and thus were very susceptible to artifacts. When these 2 patients were excluded from the analysis, the false positive rate dropped to 0.39 fp/h.
A variety of detected seizures are given in figures 11 and 12.

(Fig. 11 here)
(Fig. 12 here)

In general, for both algorithms, long, high-amplitude seizures are rarely missed. The algorithms' sensitivity is lowest for subtle, short seizures which lack repetitiveness (arrhythmic) (Fig. 13). Finally, Fig. 14 provides a few examples of false positive detections of extra-cerebral activity of biological origin; Fig. 15 shows some false positives caused by non-biological external sources. The ECG artefact was very dominant and present throughout the recording in a few patients. To deal with this artefact we developed an ECG reduction algorithm based on Independent Component Analysis (ICA) and applied it to the EEG before the seizure detection algorithm was run (a detailed description of this algorithm is out of the scope of this paper). This greatly improved the false positive rate, but in spite of this step, the ECG artefact remained responsible for some false positives.

(Fig. 13 here)
(Fig. 14 here)
(Fig. 15 here)

4. Discussion

In this paper, we introduced a new approach to detecting neonatal seizures. Our approach is based on the two major characteristics of seizures (repetitiveness and a change relative to the background) that a human observer seems to employ. Although all seizures share these properties, their appearance can be very different (continuous versus discontinuous, low versus high frequency. Close observation, however, led to the identification of two types and, consequently, the development of two detection algorithms (Fig. 16).

(Fig. 16 here)

For that purpose, we used several concepts that were previously introduced in the literature (autocorrelation, NLEO, and wavelets), but we improved and combined them, while adding some of our own concepts. For example, just like Liu et al. (1992), we make use of the autocorrelation – but we only use it to detect seizures with a continuous type of repetitiveness. Furthermore, instead of analyzing the autocorrelation of the complete EEG, we limit the analysis to those parts of the signal that represent an important increase of low-frequency activity relative to the background. The combination of these improvements dramatically decreases the number of false positive detections without altering the sensitivity.
A novel property of the spike train detection algorithm is its ability to detect repetitive segments of EEG even when two neighboring seizure segments are interrupted by other EEG activity (Fig. 6). This adaptive, segmentation-based detection is much more flexible than analyzing a fixed epoch of EEG (like classifier-based approaches do). It is known that neonatal seizures are extremely variable in morphology and frequency (Lombroso, 1996; Shewmon, 1990), which makes it very difficult to develop a patient-independent algorithm. To deal with this variability, it is important to develop a data-driven algorithm that either derives its thresholds from the data or uses parameters that are independent of the variability. For instance, in our approach, the thresholds for the segmentation of the EEG in the spike train detection are derived from the data ('q3' and 'std' of the amplitude). Similarly,

in the oscillation detection, the algorithm references to the background EEG. The remaining fixed thresholds are the correlation between the segments and the features derived from the autocorrelation. However, these parameters are independent of the variability of the seizures, because they only exploit the repetitiveness of the seizures and are independent of the actual seizure shape.

The sensitivity of the combined algorithms was good (*SensT_PP* 85%, *SensT* 88%) at a practically acceptable false positive rate of 0.66 fp/h and mean PPV of 75%. For comparison, the algorithm by Navakatikyan et al. (2006) reported sensitivities of 83-95%. PPV of 48-77% and 2 fp/h. The algoritms of Gotman (1997) and Liu were also evaluated by Navakatikyan et al. In their evaluation, the sensitivity of the Gotman algorithm ranged between 39.3 and 87.9%, and for the Liu algorithm between 97.9 and 99.2%. However, the false positive rate for the Gotman algorithm ranged from 7.4 to 10.4 fp/h, and an even higher 15.7 fp/h for the Liu algorithm. Faul et al. (2005) have also evaluated the performance of the Liu and Gotman algorithms. The reported a sensitivity of 62.5% for the Gotman algorithm and 42.9% for the Liu algorithm. Unfortunatly, no fp/h measure was given.

During validation of our methodology, we regularly encountered rhythmic activity in the EEG, detected by the algorithm, of which the non-cerebral origin of the EEG activity was not always clear, even for the neurologist, by only using the information from the scalp electrodes. In those cases, additional information from the simultaneously recorded polygraphic channels of ECG, respiration, movement sensor or even video were needed to establish that the activity present in the EEG was cerebral in nature or caused by an external source. To decrease the false positive rate of our algorithm further, these signals will have to be included in the analysis, as it is impossible to correctly classify them based on EEG analysis alone. At this point, we have only included the simultaneously recorded ECG in our analysis, by performing an ECG reduction on the data before the seizure detection algorithm was run.

The present parameter settings are for offline analysis and to obtain maximum sensitivity at an acceptable false positive rate. In a monitoring environment it might be desirable to obtain a lower false positive rate at the cost of a lower sensitivity. For the spike train type detection algorithm this can be achieved by increasing the threshold on the correlation between the detected segments. For the oscillatory type detection the threshold on the skewness and the allowed percentage difference between the zero crossings may be decreased. By tuning these parameters we believe the algorithm to be suitable for online monitoring with sufficient sensitivity and practical false positive rate. The dataset on which the algorithm was tested consisted only of full-term neonates with perinatal asphyxia. In the future we would like to test it on preterm neonates. Nevertheless, the fact that our algorithm demonstrates a high sensitivity in the presence of all possible types of background activity suggests that it may also perform well on other kinds of EEG, including preterm EEG.

5. References

Aarabi A, Wallois F, Grebe R. Automated neonatal seizure detection: A multistage classification system through feature selection based on relevance and redundancy analysis. Clin Neurophysiol, 2006;117:328-340.

Agarwal R, Gotman J, Flanagan D, Rosenblatt B. Automatic EEG analysis during long-term monitoring in the ICU. Electroenceph clin Neurophysiol, 1998;107:44-58.

Celka P, Colditz P. A computer-aided detection of EEG seizures in infants: a singular spectrum approach and performance comparison. IEEE transactions on biomedical engineering, 2002;49(5):455-462.

Clancy RR, Legido A, Lewis D. Occult neonatal seizures. Epilepsia, 1988;29:256-261.

Faul S, Boylan G, Connolly S, Marnane L and Lightbody G. An evaluation of automated neonatal seizure detection methods. Clin Neurophysiol, 2005;116:1533-1541.

Gotman J, Flanagan D, Zhang J, Rosenblatt B, Automatic seizure detection in the newborn: methods and initial evaluation. Electroenceph clin Neurophysiol, 1997; 103:356-362.

Greene BR, Boylan GB, Reilly RB, de Chazal P, Connolly S. Combination of EEG and ECG for improved automatic neonatal seizure detection. Clin Neurophysiol, 2007;118:1348-1359.

Holmes GL, Gaiarsa JL, Chevassus-Au-Louis N, Ben-Ari Y. Consequences of neonatal seizures in the rat: morphological and behavioral effects. Ann Neurol, 1998;44:845-857.

Kaiser JF. On a simple algorithm to calculate the energy of a signal. IEEE International Conference on Acoustics, Speech, and Signal Processing (ICASSP90), 1990;381-384.

Koh S, Storey TW, Santos TC, Mian AY, cole AJ. Early-life seizures in rats increase susceptibility to seizure-induced brain injury in adulthood. Neurology, 1999;53:915-921.

Liu A, Hahn JS, Heldt GP, Coen RW. Detection of neonatal seizures through computerized EEG analysis. Electroenceph clin Neurophysiol, 1992;82:30-37.

Liu Z, Yang Y, Silveria DC, Sarkisian MR, Tandon P, Huang LT, Stafstrom CE, Holmes GL. Consequences of recurrent seizures during early brain development. Neuroscience, 1999;92:1443-1454.

Lombroso CT. Neonatal seizures: a clinician's overview. Brain Dev, 1996;18:1-28.

McBride MC, Laroia N and Guillet R. Electrographic seizures in neonates correlate with poor neurodevelopmental outcome. Neurology, 2000;55:506-514.

Navakatikyan MA, Colditz PB, Burke CJ, Inder TE, Richmond J and Williams CE. Seizure detection algorithm for neonates based on wave-sequence analysis. Clin Neurophysiol, 2006;117:1190-1203.

Patrizi S, Holmes GL, Orzalesi M, Allemand F. Neonatal seizures: characteristics of EEG ictal activity in preterm and fullterm infants. Brain Dev, 2003;25:427-437.

Plotkin EI, Swamy MNS. Nonlinear signal processing based on parameter invariant moving average modeling. In Proc. CCECE'21, 1992;TM3.11.1-TM3.11.4.

Schmid R, Tandon P, Stafstrom CE, Holmes GL. Effects of neonatal seizures on subsequent seizure-induced brain injury. Neurology, 1999;53:1754-1761.

Shellhaas RA, Clancy RR. Characterization of neonatal seizures by conventional EEG and single-channel EEG. Clin Neurophysiol, 2007;118:2156-2161.

Shewmon DA. What is a neonatal seizure? Problems in definition and quantification for investigative and clinical purposes. J Clin Neurophysiol, 1990;7:315-368.

Volpe J. Neurology of the newborn. 4the ed. Philadelphia: WB Saunders, 2001.

Zarjam P, Mesbah M, Boashash B. An optimal feature set for seizure detection systems for newborn EEG signal. ISCAS(5), 2003;33-36.

List of tables and figures

Tables

Table1: Results of the combined algorithms. Patient 22 to 26 were seizure-free. (rec. len. is recording length)

Figures

Fig. 1: A: Example of a spike train type seizure, B: Example of an oscillatory type seizure, C: Example of a seizure consisting of both seizure types. The seizure starts with oscillatory activity and ends with a spike train.

Fig.2: Segmentation of a spike train seizure. After segmentation only the highest energy segments of the EEG remain. Each spike is isolated into a separate segment.

Fig.3: Definition of the background when calculating the spikiness of a segment.

Fig.4: Analysis of the correlation between the segments. In case of a repetitive pattern a set of highly correlated segments is grown.

Fig.5: The search back for correlated segments is limited to 40 times the length of the first segment the process started with.

Fig.6: Example of the spike train detection. The marked segments are those that are detected as being part of a spike train type seizure.

Fig.7: The gray blocks represent detected changes in specific wavelet scales. It can easily be seen that these represent an increase of activity relative to the preceding signal.

Fig.8: Difference between the autocorrelation functions (A' and B') of a non-repetitive (A) and repetitive signal (B).

Fig.9: The intervals between the zero crossings of the autocorrelation (B) of a repetitive signal (A) are regular. The arrows indicate which intervals are compared (each interval is used twice).

Fig.10: A: Result of the oscillation detection algorithm. The shaded areas show that the beginning of the seizure is correctly detected, whereas the last part on channels Fp1-F3, F3-C3 and C3-P3 is not, B: Result of the spike train detection algorithm. The shaded areas show that the last part of the seizure, which was not detected by the oscillation detection algorithm (Fig. 13), is correctly detected by the spike train detection algorithm. The combination of both algorithms yields a complete detection.

Fig.11: Seizures detected by the spike train detection algorithm. A: the onset of a high amplitude and long spike train type seizure, B: short, low-amplitude spike train, C: short, high-amplitude spike train.

Fig.12: Seizures detected by the oscillatory detection algorithm. A: high-amplitude oscillation, B: high-amplitude oscillation, but less rhythmical than example A.

Fig.13: Examples of missed seizures. A: high-amplitude, arrhythmic oscillatory seizure, B: short, low-amplitude spike train (complete seizure is shown). C: short, focal, high-amplitude seizure (complete seizure is shown).

Fig.14: Examples of false detections of biological origin. A: ECG artefact, B: tremor artefact, C: pathological fast eye movements (nystagmus).

Fig.15: Examples of false positive detections of non-biological origin. A: high-frequency artifact, due to the heating of the bed, B: ventilation artifact, as shown by the high correlation with a sensor on the abdomen.

Fig.16: Schematic overview of the complete algorithm.

Figure 1

Click here to download high resolution image

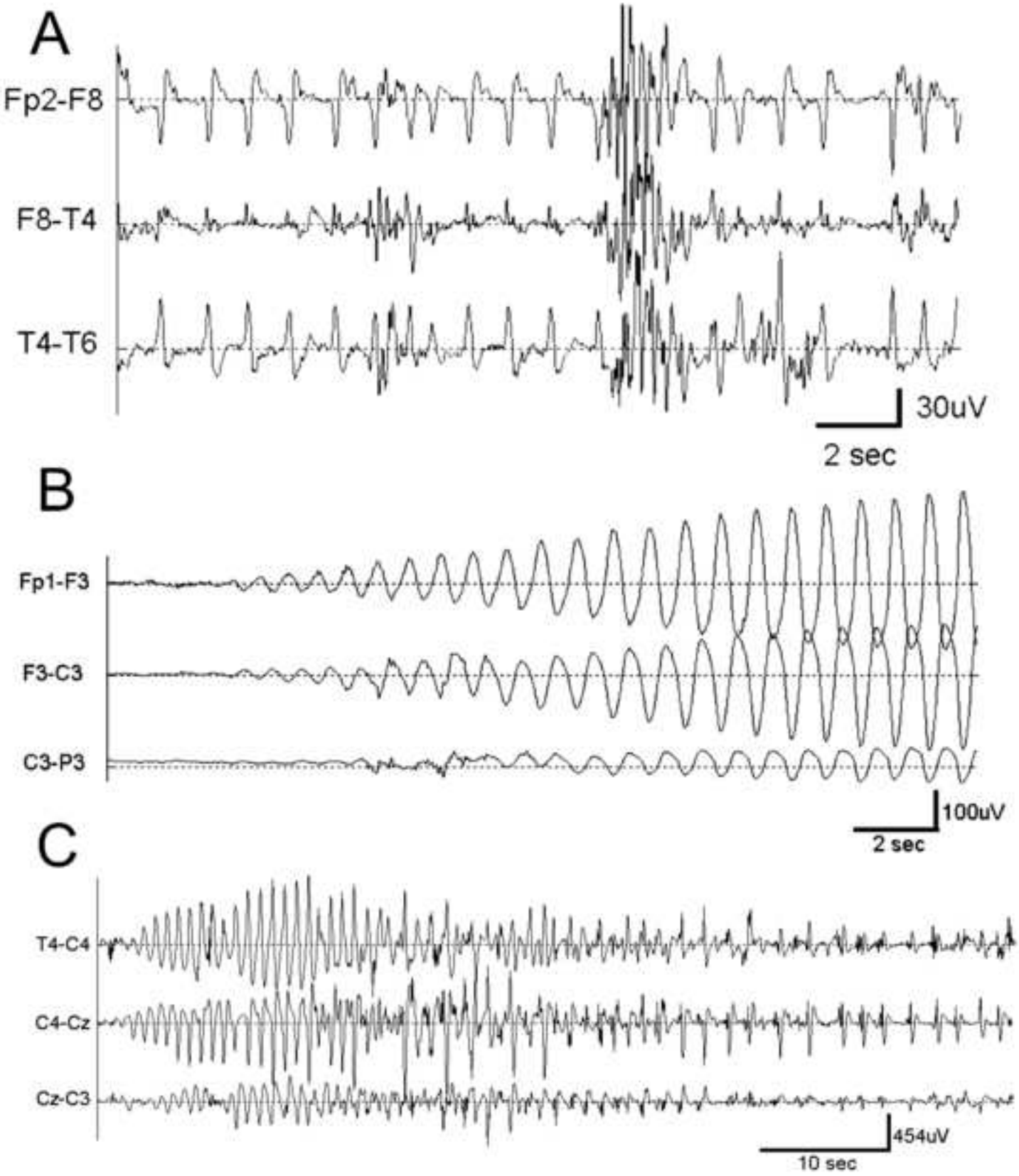


Figure 2

Click here to download high resolution image

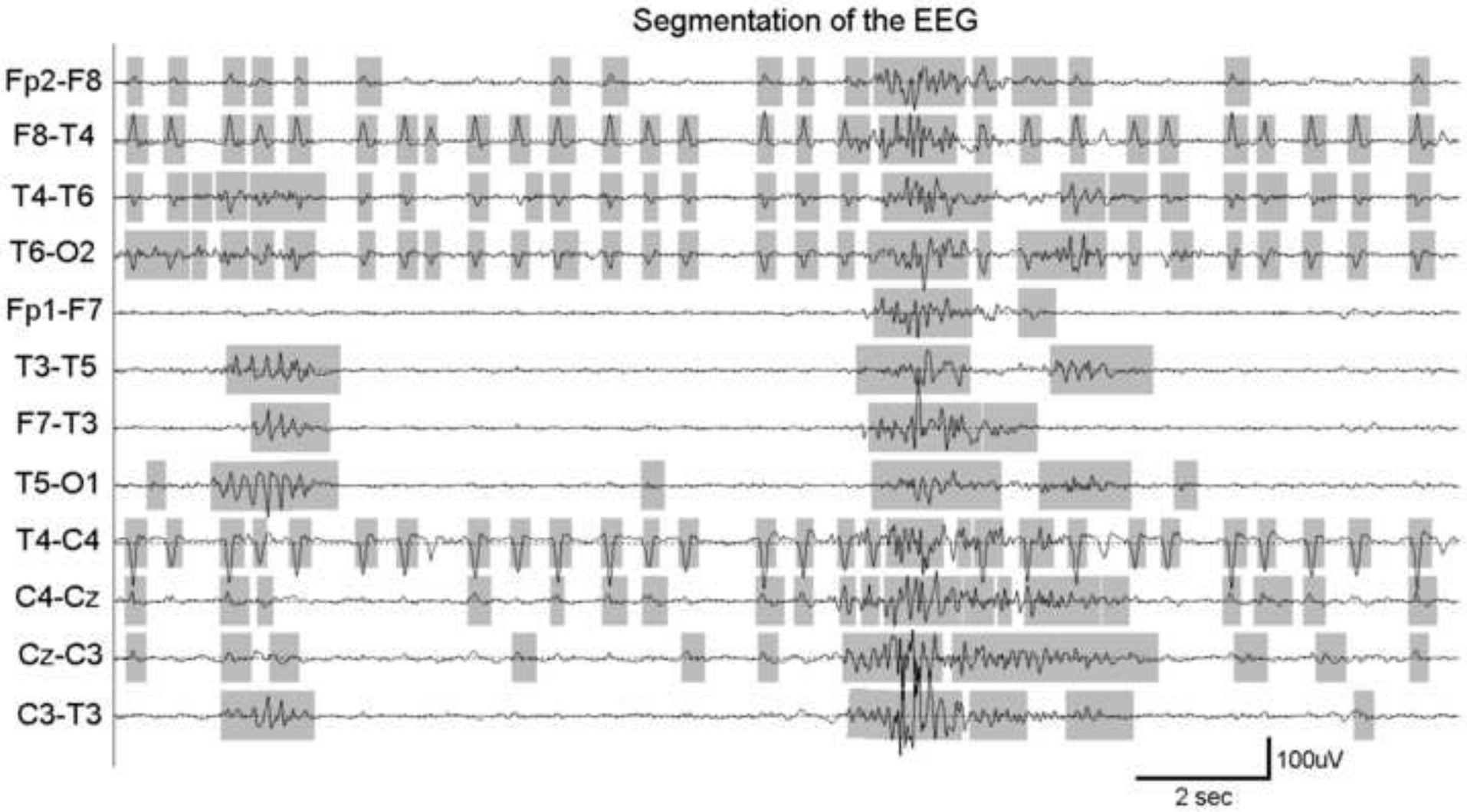


Figure 3

Click here to download high resolution image

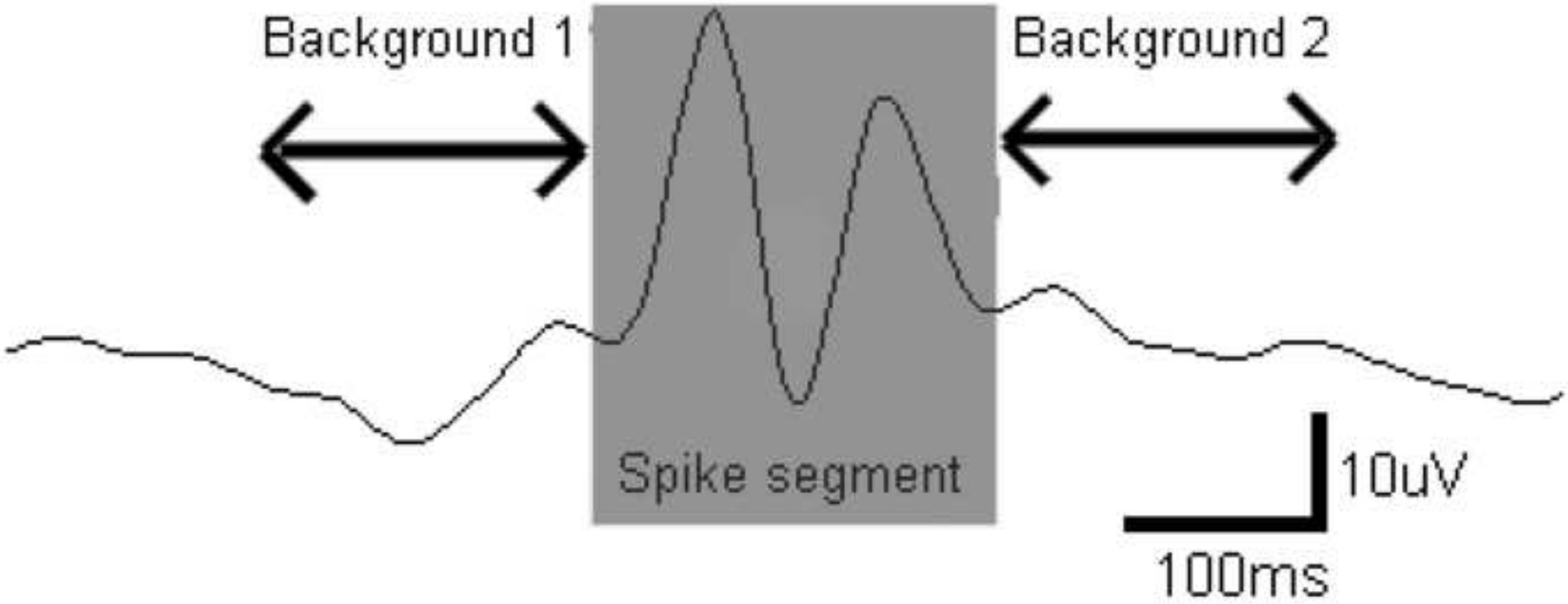


Figure 4
Click here to download high resolution image

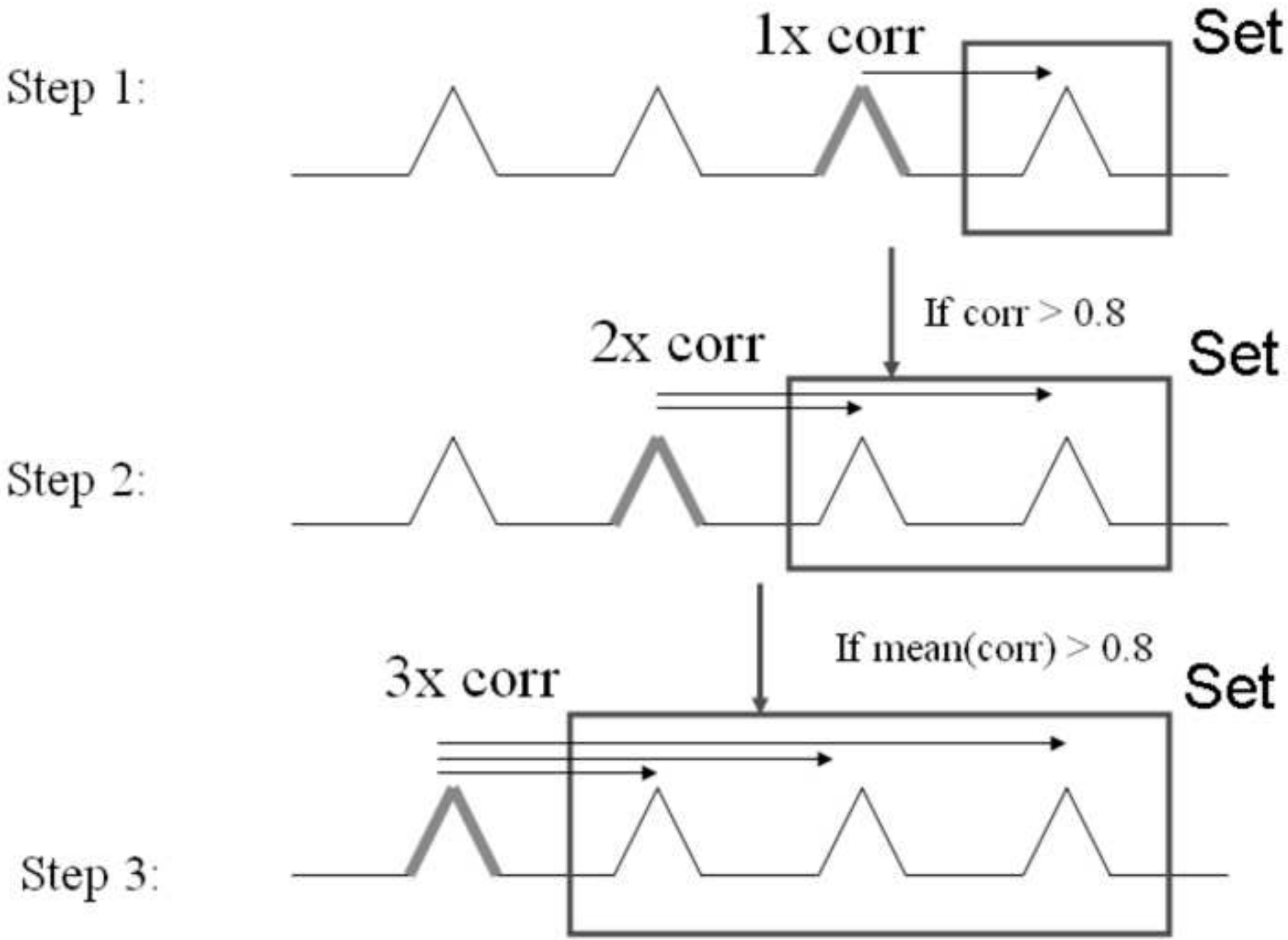


Figure 5
Click here to download high resolution image

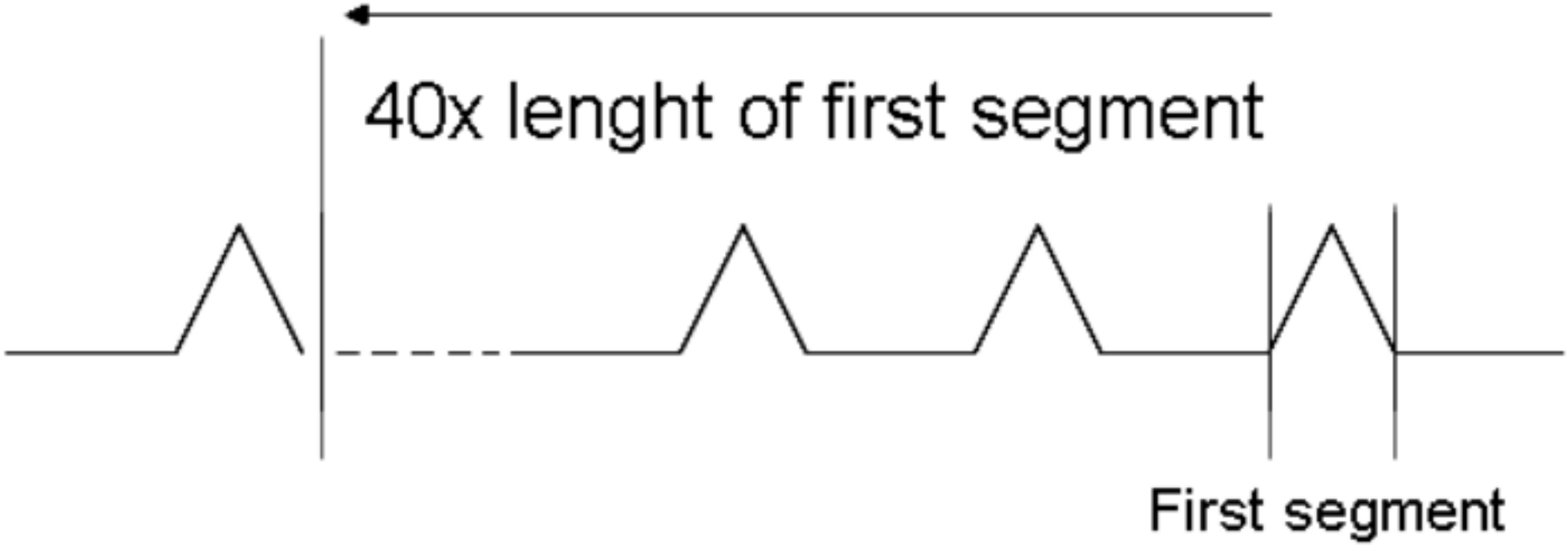


Figure 6

Click here to download high resolution image

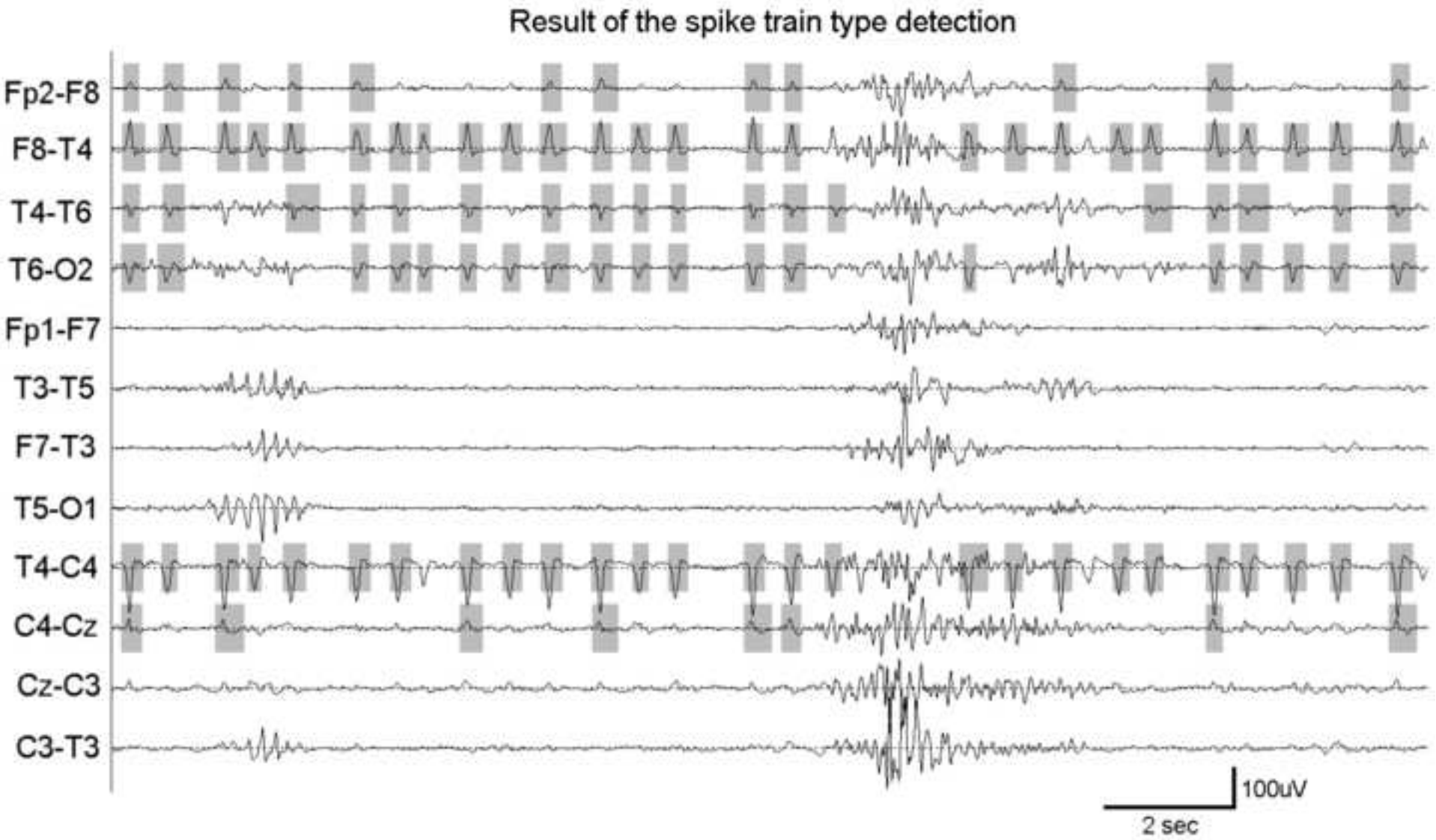


Figure 7

Click here to download high resolution image

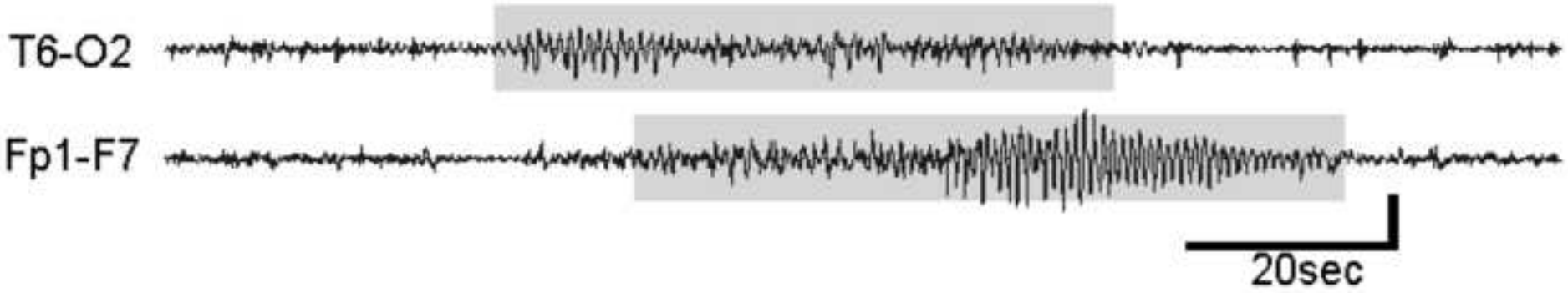


Figure 8

Click here to download high resolution image

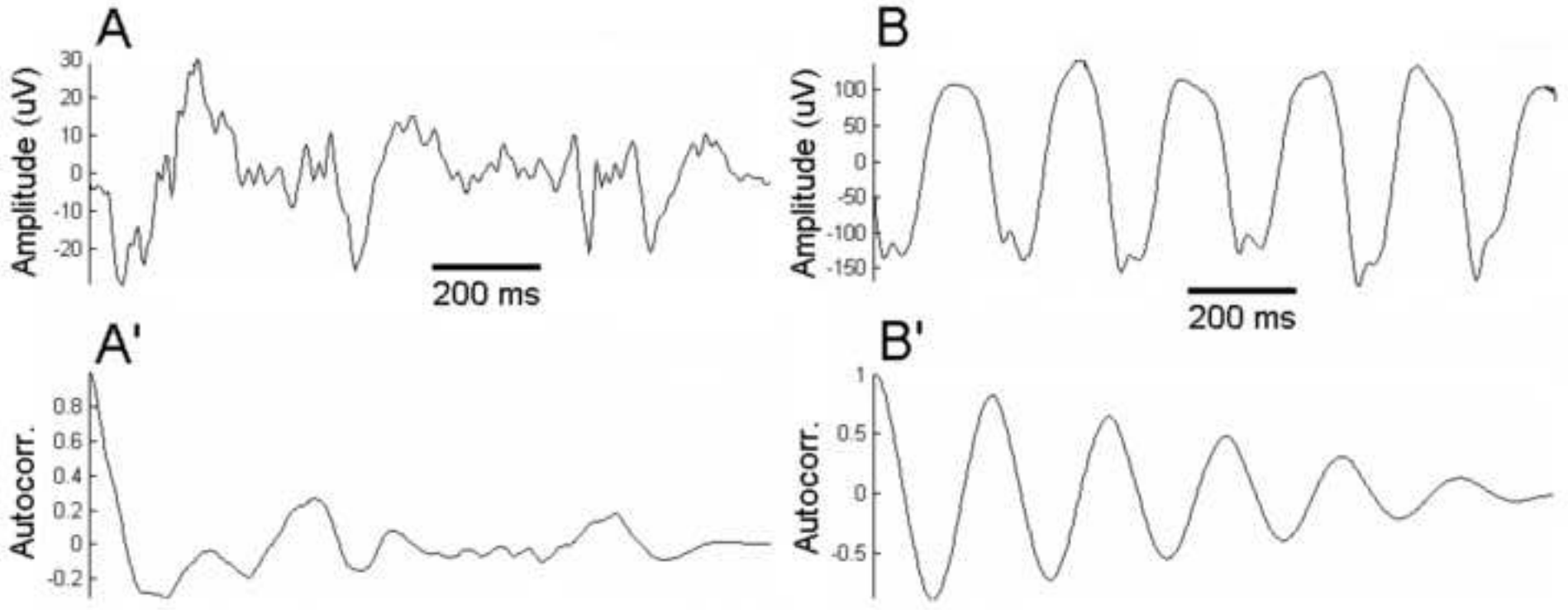


Figure 9

Click here to download high resolution image

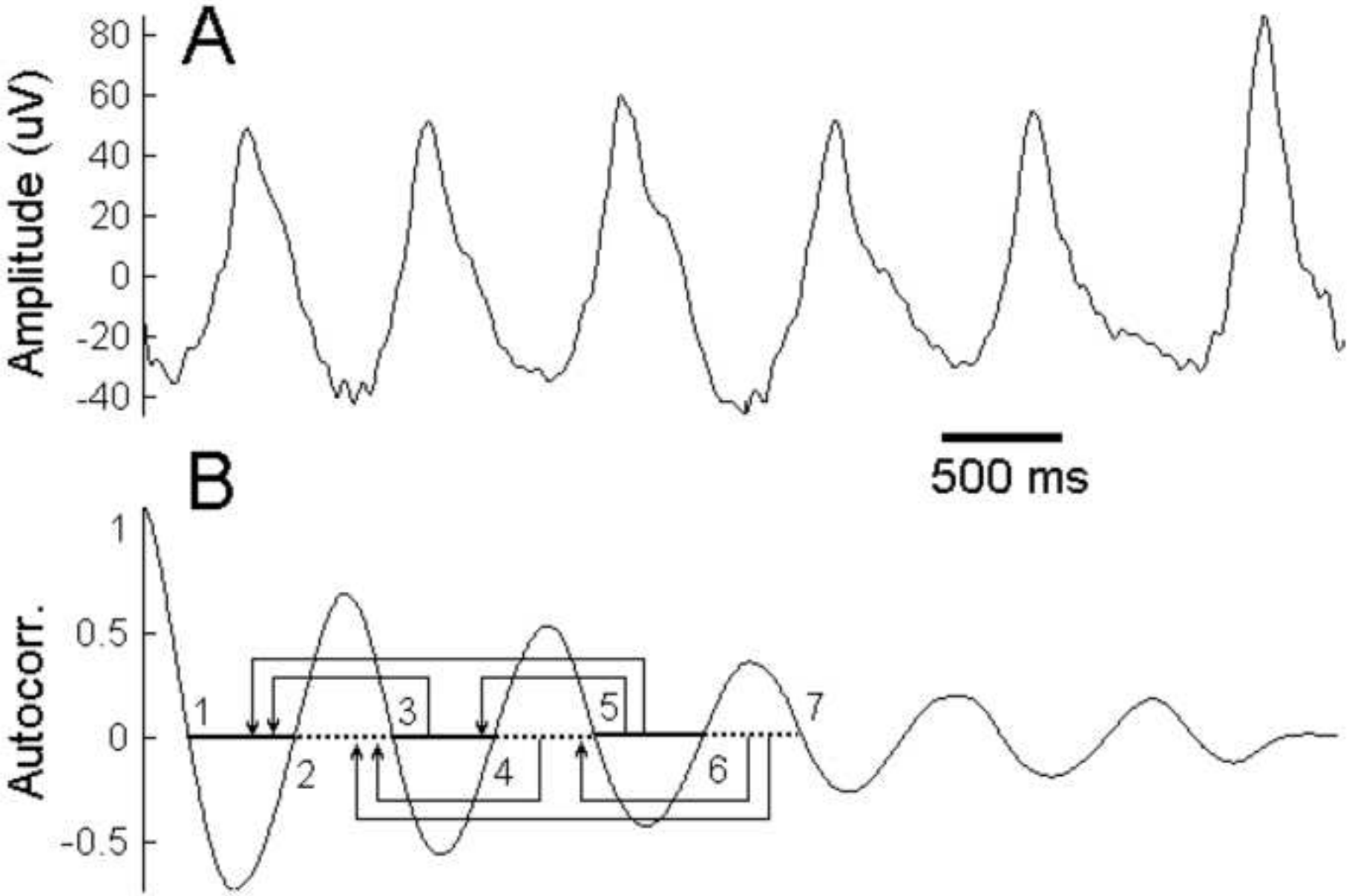


Figure 10

Click here to download high resolution image

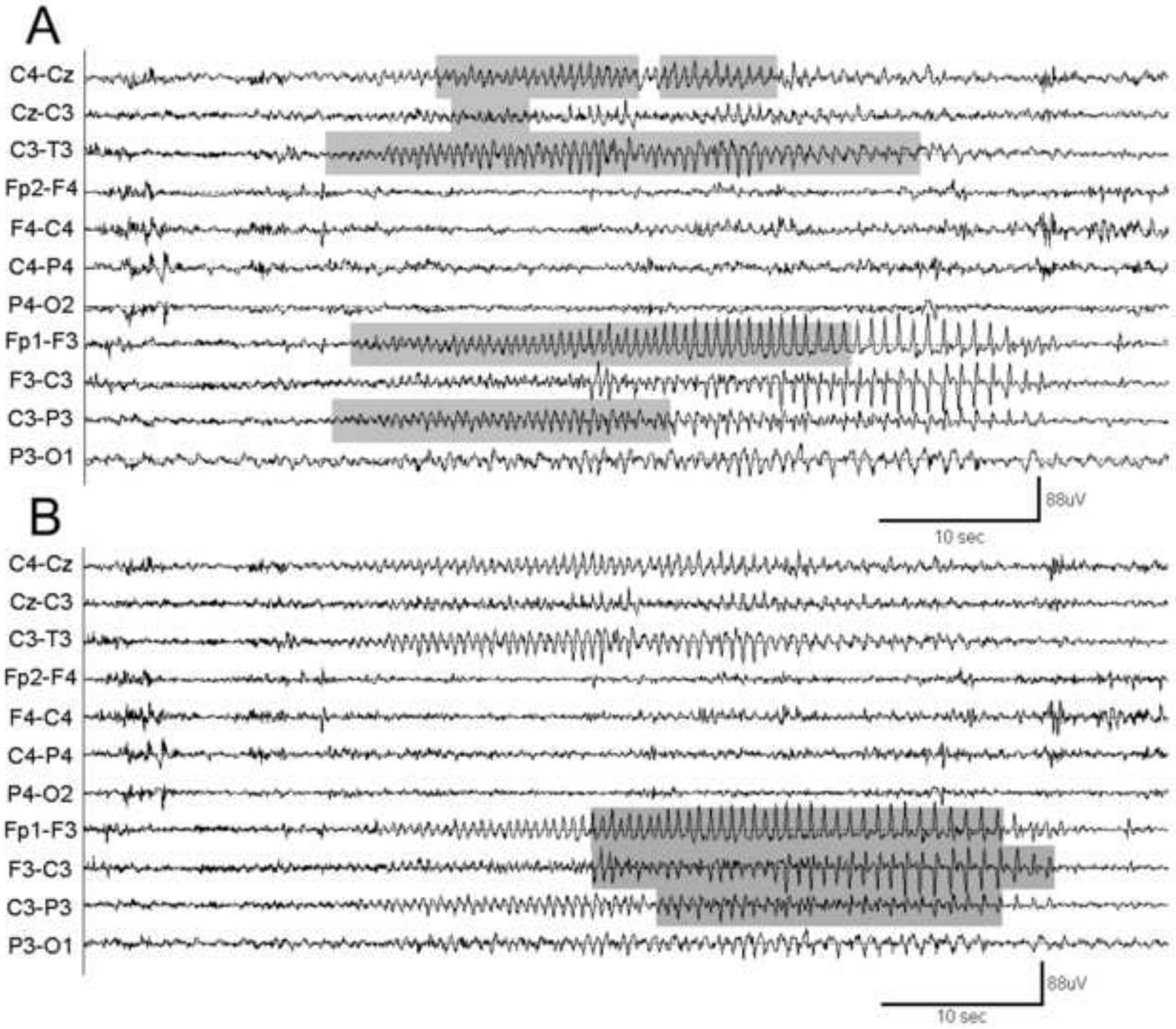


Figure 11

Click here to download high resolution image

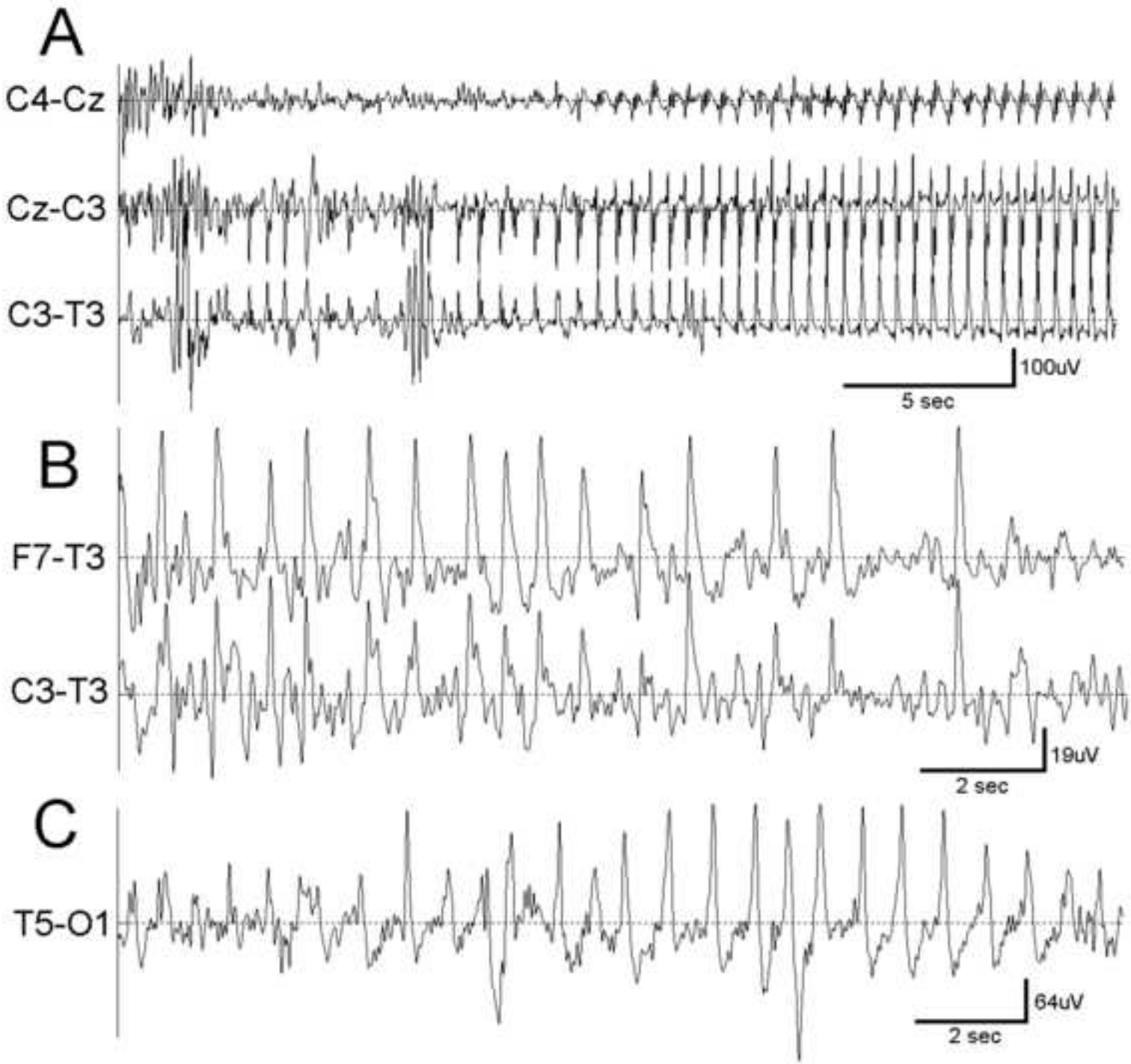


Figure 12

Click here to download high resolution image

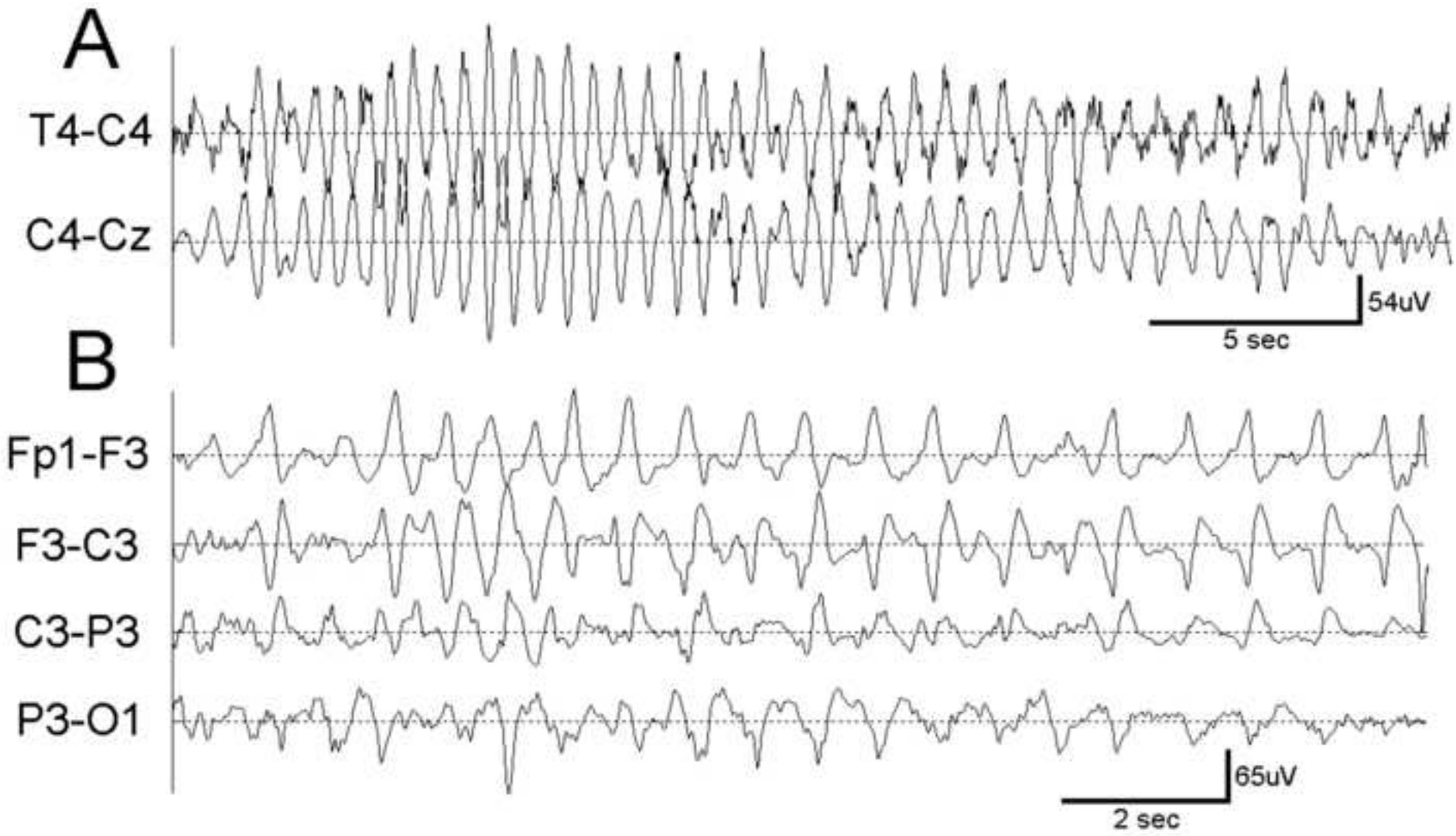


Figure 13

Click here to download high resolution image

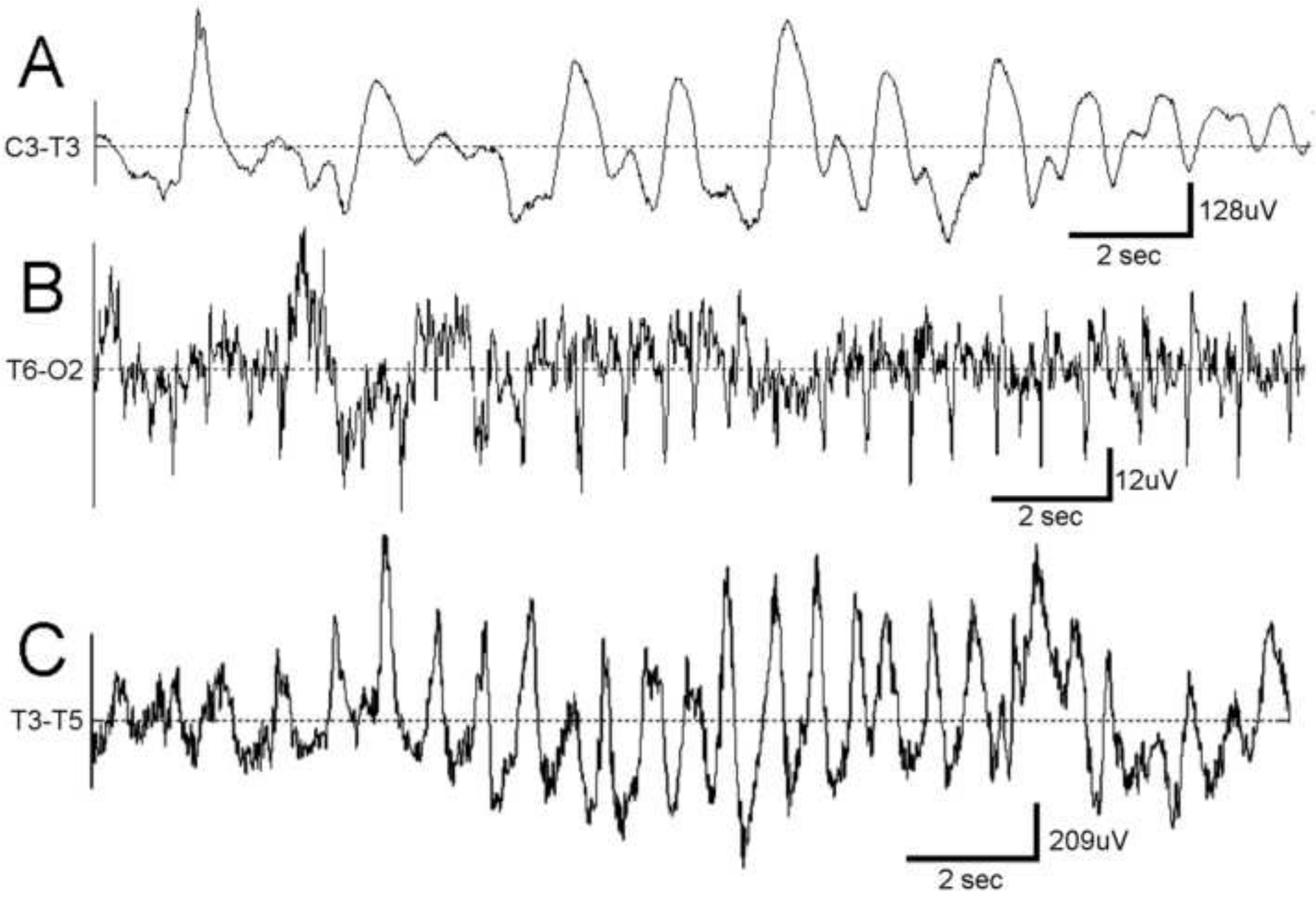


Figure 14

Click here to download high resolution image

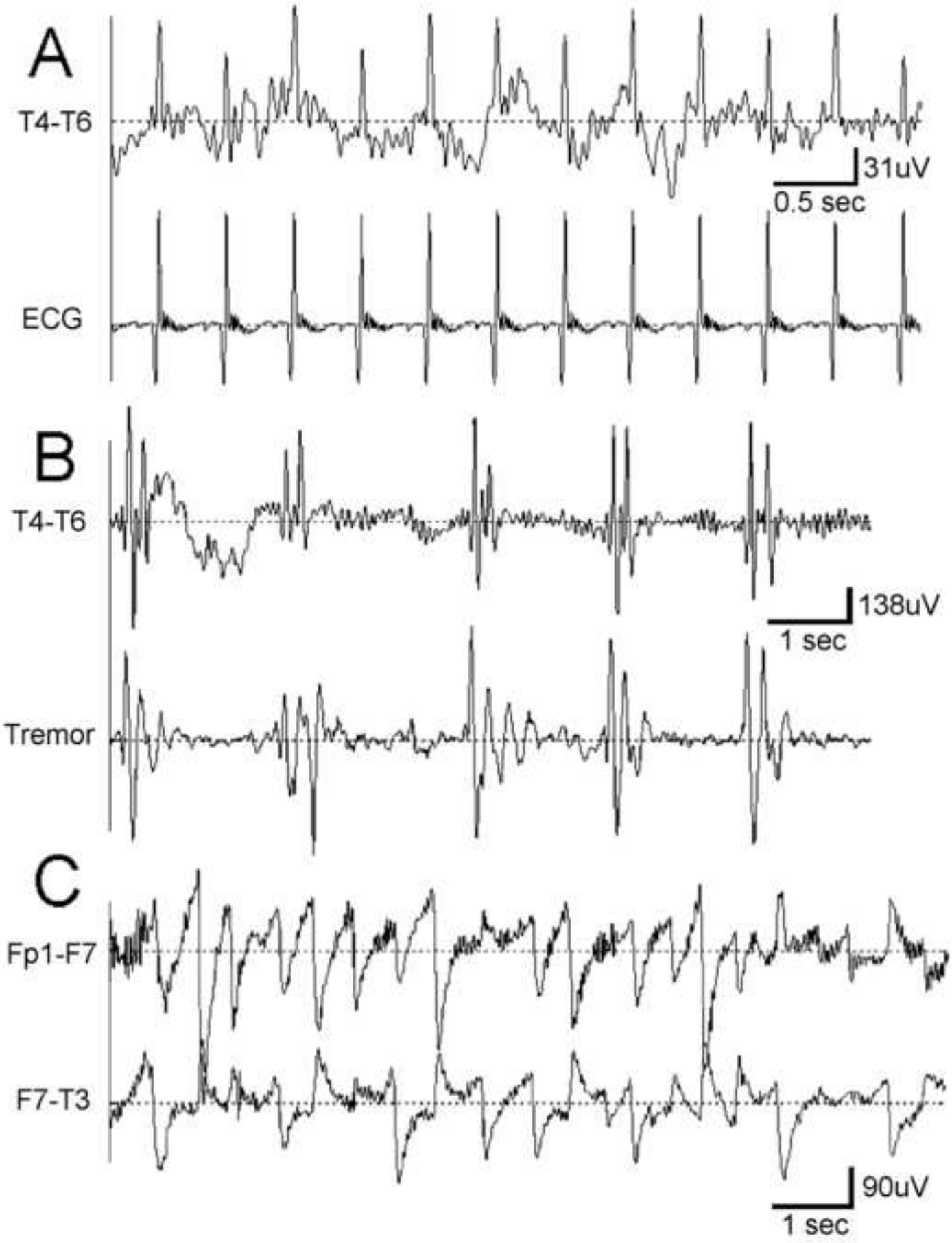


Figure 15

Click here to download high resolution image

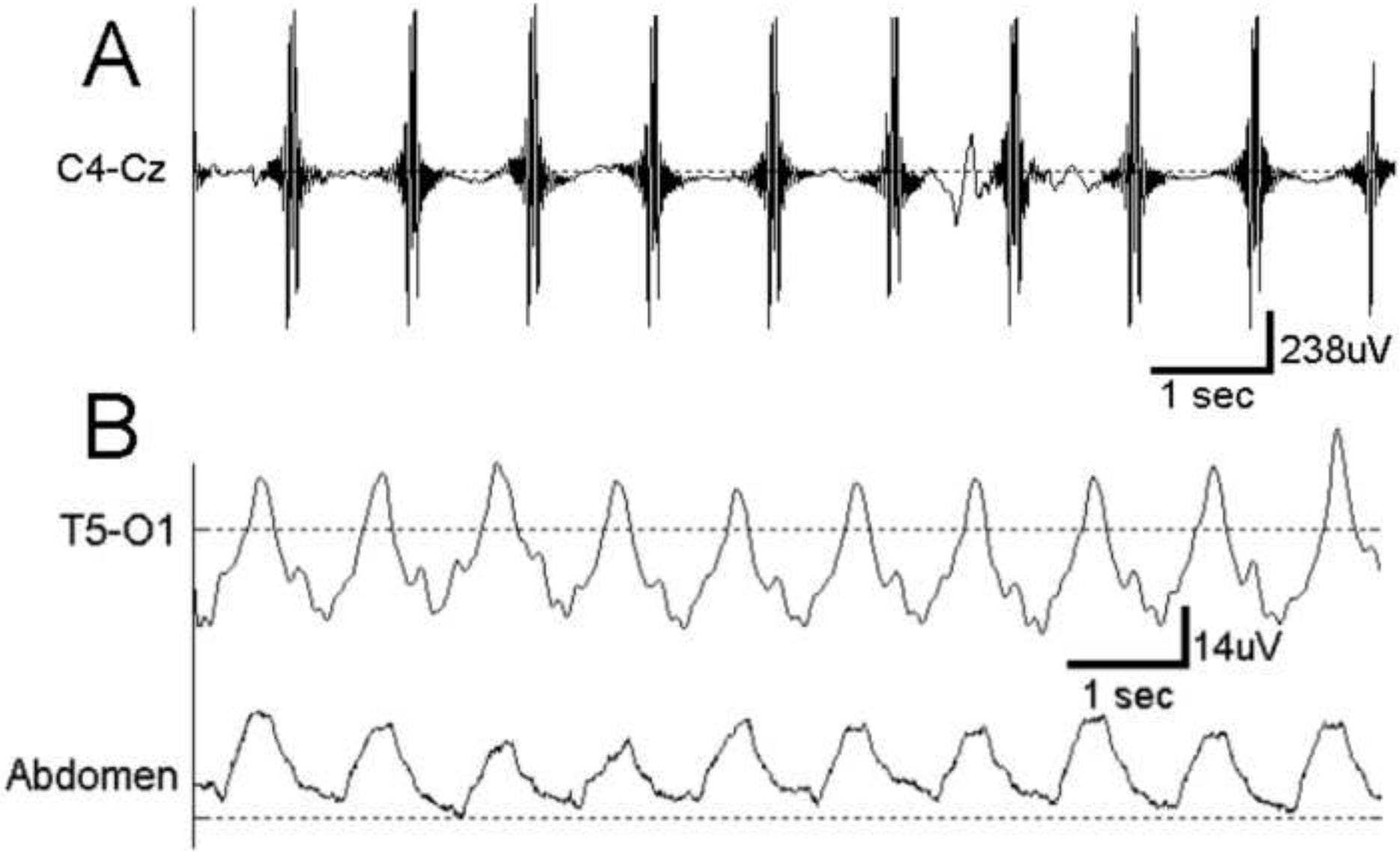


Figure 16

Click here to download high resolution image

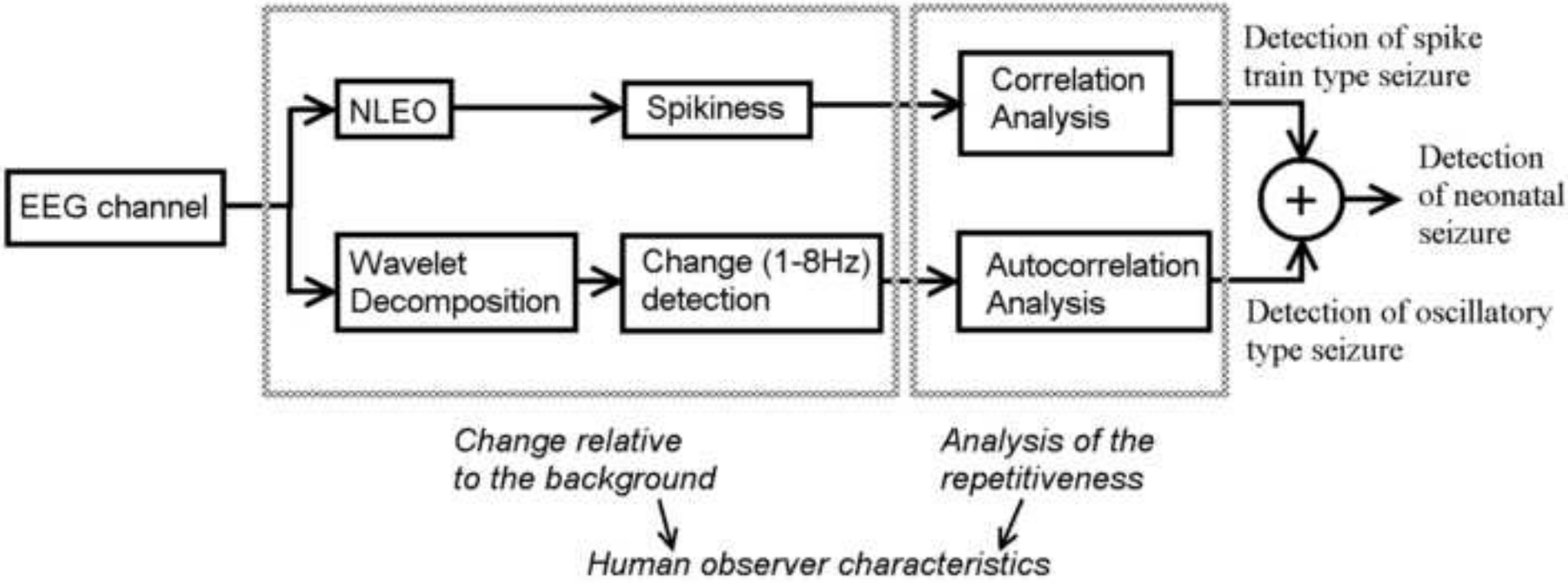


Table1

id number	SensPP (%)	PPV (%)	fp/h	rec. len. (h)
1	92	94	0.51	7.9
2	100	32	1.65	7.9
3	92	65	1.52	7.9
4	90	72	1.27	7.9
5	100	80	0.13	7.9
6	90	100	0.00	7.9
7	89	60	4.05	7.9
8	82	64	0.63	7.9
9	100	100	0.00	7.9
10	100	90	0.13	7.9
11	100	33	0.51	7.9
12	100	90	0.25	7.9
13	96	85	0.51	7.9
14	96	83	0.63	7.9
15	45	71	0.25	7.9
16	50	50	0.13	7.9
17	38	89	0.13	7.9
18	86	86	0.13	7.9
19	60	75	0.13	7.9
20	100	61	1.39	7.9
21	82	100	0.00	7.9
22	x	x	0.00	20
23	x	x	4.05	7.9
24	x	x	0.13	7.9
25	x	x	0.00	7.9
26	x	x	0.00	7.9
	SensT_PP:	**85%**		
	SensT:	**88%**		
	PPV:	**75%**		
	fp/h:	**0.66**		

Author Agreement

Click here to download high resolution image

AUTHOR CONCURRENCE FORM

CLINICAL NEUROPHYSIOLOGY

Official Organ of the International Federation of Clinical Neurophysiology

http://www.elsevier.com/clinph

Prof. David Burke, Editor-in-Chief

Instructions:

1. Each submission to Clinical Neurophysiology needs a filled out Author Concurrence Form. Please fill in the Title of the manuscript.
2. Collect signatures from all authors.
3a. Scan the form and submit it together with the paper. The submission item is Author Agreement.
3b. If this is not an option, please fax the form to the Editorial Office: +31-20-485-3881.

Title of the Manuscript: Automated neonatal seizure detection mimicking a human observer reading EEG

A signature below certifies compliance with the following statements.

Copyright Transfer: In consideration of the acceptance of the above manuscript for publication, the copyright is transferred to IFCN and administered by Elsevier. All proprietary rights other than copyright (such as patent rights) are reserved to the author, as well as the right to use original figures and tables in future works, provided full credit is given to the original publication. If the manuscript is work prepared by employee(s) of the United Kingdom or the United States government as part of their official duties, copyright cannot be fully transferred to the IFCN, and authors must check the appropriate box below.

- This manuscript was written in the course of employment by the United Kingdom and it is subject to Crown copyright.
- This manuscript was written in the course of employment by the United States Government and it is not subject to copyright in the United States.

Authorship Responsibility: The submission is a truthful, original work without fabrication, fraud or plagiarism, and contains no libellous or unlawful statements.

It has not been published previously except in abstract form.

The manuscript is not under consideration for publication, nor will it be submitted for publication, elsewhere until a final decision has been made by this journal.

The undersigned certify that each has participated sufficiently in the work to take responsibility for its truthfulness and validity and has read the complete manuscript.

Conflict of interest disclosure: All funding sources supporting this work are acknowledged. The authors will disclose to the editor any pertinent financial interests associated with the manufacture of any drug or product described in this manuscript.

ALL AUTHORS MUST SIGN

Author: W. Deburchgraeve _____ Date 25-03-2008

Author: P.J. Cherian _____ Date 17-03-2008

Author: M. De Vos _____ Date 25/03/08

Author: R.M. Swarte _____ Date 18-03-2008

Author: J.H. Blok _____ Date 17.03.2008

Author: G.H. Visser _____ Date 18-3-2008

Author: P. Govaert _____ Date 19/03/08.

Author: S. Van Huffel _____ Date 24/3/08